



## THE INFLUENCE OF THE REACTIVE ELEMENT YTTRIUM ON THE STRESS IN ALUMINA SCALES FORMED BY OXIDATION

R. J. CHRISTENSEN, V. K. TOLPYGO and D. R. CLARKE

Materials Department, College of Engineering, University of California, Santa Barbara, CA 93106-5050,  
U.S.A.

(Received 13 March 1996)

**Abstract**—The addition of reactive elements, such as yttrium, to high temperature alloys significantly improves the adherence of thermally-grown oxide scales but there is still no agreement as to the reason for this improved behavior. Some of the proposed mechanisms are based on the premise that yttrium helps to decrease the residual compressive stress in the oxide, thus decreasing the driving force for spalling of the oxide scale. This investigation followed the oxide stress development in three alumina-forming alloy compositions, each with and without an addition of yttrium over various oxidation times and temperatures. The stress in the oxide scales were measured at room temperature using a piezospectroscopic technique. The results clearly show that the addition of yttrium does not decrease the residual stress in the scales but makes them more compressive, at least at short oxidation times. © 1997 Acta Metallurgica Inc.

### 1. INTRODUCTION

About 60 years ago, it was discovered [1] that the addition of small amounts of reactive or rare earth elements (such as yttrium, hafnium, and cerium) to an alloy resulted in substantial improvements in the adherence of their oxide scales during thermal cycling as measured by the resistance to spalling of the scale. The improved spall resistance has come to be termed the reactive element effect and is now exploited in almost all high temperature alloys, whether they be alumina or chromia forming alloys [2]. Despite a considerable body of research [3–24] over several decades the origin of the improved spall resistance [3–24] is far from understood although several hypotheses have been proposed to explain the origin of the reactive element effect.

Part of the difficulty in identifying the mechanism(s) responsible for the reactive element effect is the wide variety of microstructural effects reactive elements have on the oxide scale and the underlying metal. The microstructural variations have been studied most widely with yttrium as the prototypical reactive element. For instance, the addition of yttrium to an alumina forming alloy commonly results in an  $\alpha$ -Al<sub>2</sub>O<sub>3</sub> scale that tends to be very flat with the absence of voids at the interface [2–6, 15–17, 20, 23], whereas the yttrium-free alloys tend to form a convoluted scale with interface voids [2–7, 15, 23]. Yttrium also tends to promote a columnar grain structure of aluminum oxide scales with a reported finer grain size as compared to the equiaxed grains of the yttrium-free material [6, 17].

Yttrium has also been found to favor O<sup>2-</sup> diffusion through oxide grain boundaries over Al<sup>3+</sup> diffusion through the oxide grains, such that new oxide forms preferentially at the interface [6, 14]. On the basis of observations such as these as well as the increased resistance to spalling several mechanisms for the improved oxide adherence associated with yttrium additions have been proposed. The major hypotheses include (a) increased oxide scale plasticity due to the presence of yttrium, (b) the formation of a buffer layer at the interface, (c) modification of the oxide scale growth process leading to lower stresses in the scale, (d) improved chemical bonding at the interface, (e) prevention of void growth at the interface by formation of alternative vacancy sinks in the alloy, (f) formation of pegs in the oxide at the interface to help mechanically anchor the oxide in place [7], and (g) the tying up of segregants into stable compounds preventing segregation to the oxide/metal interface which may weaken the interface [13].

The improved adherence associated with the three mechanisms (a), (b), and (c) above is generally based on the assumption that yttrium decreases the stress in the oxide scale or promotes accommodation of the oxide growth stresses [7]. For this reason there have been a number of measurements made by both X-ray diffraction [2, 12, 24] and beam deflection [2, 9, 25] techniques in order to elucidate the evolution of the stress in the oxide scales. These methods have proved to be difficult and time-consuming and so relatively few measurements have been reported. Furthermore, as they are measurement techniques that provide a value of the stress averaged over large regions, they

cannot distinguish between regions that are fully adhered and others that are partially or fully spalled. For these reasons, as well as to contribute to a fuller understanding of the role of the reactive elements, we have applied the recently developed nondestructive technique of Cr<sup>3+</sup> fluorescence piezospectroscopy [26, 27] to the measurement of the stresses in the oxide scales formed on the same composition alloys as have previously been studied by X-ray diffraction by Luthra and Briant [12] and by beam bending by Delauney *et al.* [2, 9]. These studies, on Fe–Cr–Al, Fe–Ni–Cr–Al and Ni–Cr–Al alloys, are amongst the most extensive of those reported in the literature.

## 2. EXPERIMENTAL METHODS

Three different alloy compositions were studied, each either with or without yttrium, and having the compositions listed in Table 1. (The compositions are in weight percent.) The Fe–Cr–Al alloys were prepared by induction melting and casting while the Fe–Ni–Cr–Al and Ni–Cr–Al alloys were prepared by arc-melting the components under an argon atmosphere followed by re-melting steps to ensure homogenization. Before oxidation, all samples were polished to 1  $\mu\text{m}$  diamond finish.

Oxidation was performed in a tube furnace with a heat-up rate of 10°C/min and cool-down rate of 2°C/min. The Fe–Cr–Al and Ni–Cr–Al alloys were oxidized under laboratory air while the Fe–Ni–Cr–Al alloys were oxidized under flowing oxygen. Each composition with and without yttrium was oxidized under the same conditions.

After oxidation and cooling to room temperature, the stresses in the alumina (Al<sub>2</sub>O<sub>3</sub>) scales were determined from measurements of the shift in frequency of the Cr<sup>3+</sup> fluorescence (photoluminescence), excited with a probing argon-ion laser at 514 nm, from the stress-free frequency. The full details of the measurement technique and the analysis methodology have been described in detail elsewhere [26, 27] and so only a brief description will be given here. The fluorescence originates from trace amounts of chromium incorporated into the alpha-alumina phase during the formation of the oxide scale by the oxidation of the underlying alloy. It is characterized by two distinct fluorescent transitions, known as the R-line doublet. Strain in the alumina phase gives rise to a systematic frequency shift of the R-lines, a phenomenon known as the piezospectroscopic effect. To a first-order approximation, the frequency shift,

$\Delta\nu$ , is linearly related to stress by the piezospectroscopic tensor,  $\Pi_{ij}$ :

$$\Delta\nu = \Pi_{ij}\sigma_{ij} \quad (1)$$

where  $\sigma_{ij}$  are the stress components as defined in the crystal basis. The off-diagonal terms of the piezospectroscopic tensor for chromium fluorescence in ruby have been experimentally determined to be negligible compared with the principal terms [28], significantly simplifying equation (1).

For polycrystalline alumina, such as the oxide scales formed on the alloys investigated in this work, one can assume that the probe samples a sufficient number of randomly-oriented grains to allow a reliable measurement of the average stress. By averaging equation (1) over all possible grain orientations, the resulting frequency shift is found to depend only on the hydrostatic component of the applied stress tensor and the trace of the piezospectroscopic tensor [26, 29]:

$$\Delta\bar{\nu} = \frac{1}{3}\Pi_{ii}\sigma_{ii} \quad (2)$$

where the value of the trace of the piezospectroscopic tensor  $\Pi_{ii}$  for the R-lines is 7.61 cm<sup>-1</sup>/GPa [28].

The relationship between frequency shift and stress can be further simplified by considering the symmetry of the stress state in thin oxide scales. Assuming that such scales are flat, they are in a state of biaxial compression with the stress normal to the substrate,  $\sigma_{33}$ , being equal to zero. This reduces equation (2) to:

$$\Delta\bar{\nu} = \frac{2}{3}\Pi_{ii}\bar{\sigma} \quad (3)$$

As all the fluorescence measurements were made at room temperature, the stress,  $\bar{\sigma}$ , reported in this work includes both the oxide growth stresses and the thermal mismatch stress developed between the oxide and the alloy upon cooling from the oxidation temperature. By making the measurements under an optical microscope, the stresses could be obtained from regions of the scale only a few microns across and identified in the microscope.

The frequency of the R1 and R2 lines were calibrated using a simultaneously recorded characteristic emission line from an argon lamp as a frequency standard. Since the R-line frequencies are also known to be dependent on the Cr concentration in the scale, spectra were also recorded from scales detached from the underlying metal. The frequency from the detached scale was taken to be the stress-free value used to determine the value of the stress in the adhering scale. The stress-free value determined in this manner was the same within 0.1 GPa for samples with and without yttrium.

## 3. RESULTS

### 3.1. Fe–Cr–Al alloys

The Fe–Cr–Al alloys were all oxidized at 1100°C from 0.1 to 625 h. Significant spalling did not occur

Table 1. Alloy compositions

| Composition (wt%)        | Sulphur (wt%) | Processing method |
|--------------------------|---------------|-------------------|
| Fe–22Cr–5.3Al            | 0.05          | Induction melted  |
| Fe–23Cr–4.8Al–0.03Y      | 0.004         | and cast          |
| Fe–45Ni–25Cr–5.0Al       | 0.006         | Arc-melted under  |
| Fe–46Ni–24Cr–4.8Al–0.05Y | 0.005         | Argon             |
| Ni–20Cr–12.7Al           | <0.001        | Arc-melted under  |
| Ni–20Cr–12.6Al–0.11Y     | <0.001        | Argon             |

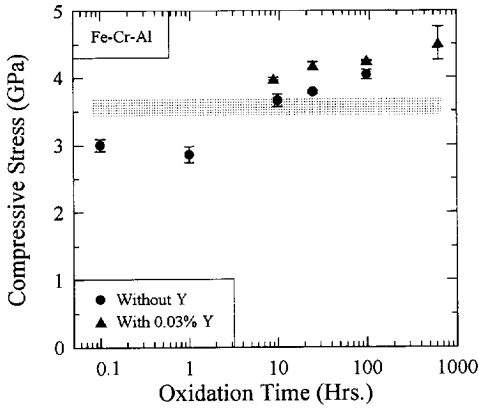


Fig. 1. Residual compressive stress, measured at room temperature, in the alpha-alumina scale formed on the Fe-Cr-Al alloy as a function of oxidation time at 1100°C in air. The shaded band in this and subsequent figures represents the range of residual stress estimated from thermal expansion mismatch alone.

for any samples with or without yttrium for the times studied. The plot of compressive stress vs oxidation time is shown in Fig. 1. In these and subsequent figures, the error bars represent the standard deviation of several measurements made at different locations on the same scale. Thus, the size of the bars provides an indication of the spatial variation in the value of the scale stress. In a number of figures the stress indicated is zero. These are measurements taken from seemingly intact scales presumably on the verge of spalling off.

The shaded band in the figure represents an estimate of the residual stress due to the thermal expansion mismatch between the oxide and the alloy for the respective alloys. Similar banded regions are also included in subsequent figures with the values determined by using the tabulated thermal expansion data of similar alloys [30] except where stated otherwise. Although the thermal expansion mismatch residual stress is straightforward to calculate there exists considerable uncertainty in the thermal expansion coefficients of the alloys. In addition, there is also some uncertainty in the modulus of the oxide scale. In evaluating the residual stress due to thermal expansion mismatch,  $\sigma_{TE}$ , the following equation was used:

$$\sigma_{TE} = \frac{E_0}{(1 - \nu_0)} \Delta\alpha\Delta T \quad (4)$$

where  $E_0$ , and  $\nu_0$ , represent the elastic modulus and Poisson's ratio of the oxide layer, assumed to be 360 GPa and 0.27, respectively. The difference,  $\Delta\alpha$ , between the coefficients of thermal expansion (CTE) of the oxide and metal,  $\alpha_0$  and  $\alpha_m$ , are the averages over the temperature difference  $\Delta T$ . The averages have been obtained from the literature except for the Fe-Cr-Al material where the averages were obtained from our own dilatometry studies.

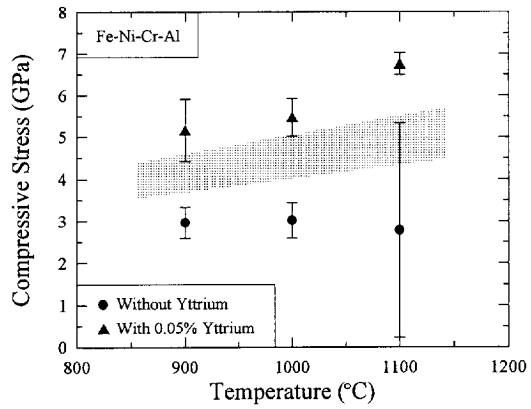


Fig. 2. Room temperature residual stress in the alpha-alumina phase of the oxide scale formed on the Fe-Ni-Cr-Al alloy after 1 h oxidation at the temperatures indicated.

3.2. Fe-Ni-Cr-Al alloys

The Fe-Ni-Cr-Al alloys were oxidized at temperatures ranging from 900° to 1100°C with oxidation time varying from 1 to 200 h. In Fig. 2, the compressive stress in the oxide scale after 1 h oxidation is plotted vs oxidation temperature. The compressive stress from oxidation at 1000°C vs oxidation time is shown in Fig. 3. The oxide scale on samples with 0.05% yttrium remained intact under these conditions while significant spalling began to occur on the samples without yttrium after 10 h at 1000°C and became progressively worse with increasing oxidation time and temperature. All data points on Figs 2 and 3 were obtained from intact scales. The scale grown on the alloy without yttrium was thicker than the scale on the yttrium-containing alloy in accordance with previous reports in the literature.

3.3. Ni-Cr-Al alloys

The Ni-Cr-Al alloys were oxidized from 950° to 1250°C for 1 to 96 h. The compressive stress in the

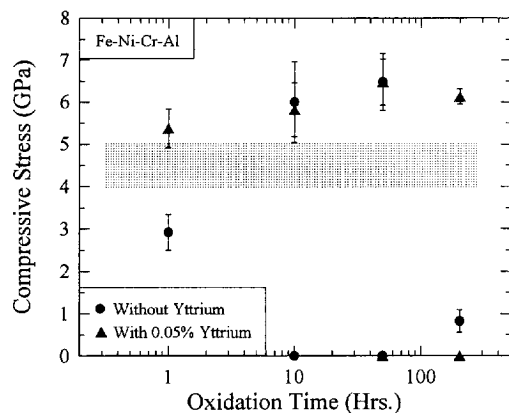


Fig. 3. Residual stress as a function of oxidation time at 1000°C. Fe-Ni-Cr-Al alloy. The data points at zero stress are from regions of the scale that remained intact.

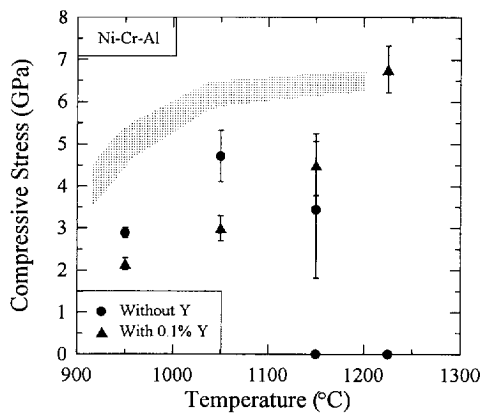


Fig. 4. Room temperature residual stress in the alumina phase formed on the Ni-Cr-Al alloy after 1 h oxidation at the temperatures indicated. The large standard deviation at 1150°C reflects the variation in the stresses noted from place to place across the scale. The change in the thermal mismatch stress is due to a phase transformation in the alloy.

oxide scale after 1 h of oxidation is plotted as a function of oxidation temperature in Fig. 4. In Fig. 5, the compressive stress in the oxide scale of the alloy with yttrium is plotted vs the oxidation time at 1150°C. Spalling was observed on all samples without yttrium, except for the samples oxidized at 950°C and 1050°C for 1 h. All stress measurements were made on intact oxide scale. The shaded band representing the thermal expansion mismatch stress was calculated using the data from Ref. [31]. The rapid change in the calculated thermal stress between 950°C and 1100°C is a result of the phase transformation at  $\sim 1000^\circ\text{C}$  that has been attributed as due to the  $\gamma + \beta \rightarrow \gamma' + \alpha$  transformation [31].

#### 4. DISCUSSION

The measurements of residual stress presented in Figs 1–5 indicate that although there is marked variation in the values of the stress from alloy to

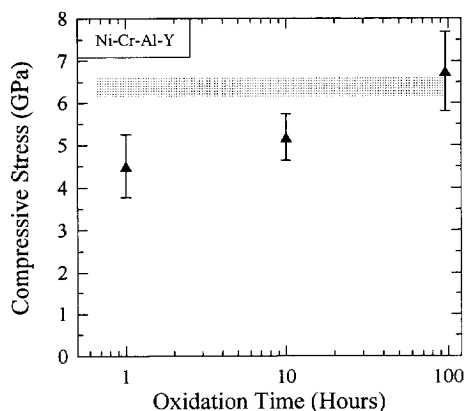


Fig. 5. Residual stress in the alpha-alumina phase on the Ni-Cr-Al-Y alloy as a function of oxidation time at 1150°C.

alloy, the effect of the reactive element yttrium is to increase the scale stress especially at early times. The effect will first be discussed separately for each alloy investigated in this study.

##### 4.1. Fe-Cr-Al alloys

The results in Fig. 1 show that the compressive stress in the oxide scale formed on Fe-Cr-Al as a function of oxidation time at 1100°C is similar with and without yttrium although the yttrium containing material sustains a larger compressive stress by about 0.7 GPa. Comparison with estimated thermal residual stress indicates that after 10 h of oxidation, residual stresses occur in the oxide on the order of 1 GPa larger than expected from thermal mismatch stress alone suggesting that there are appreciable compressive growth stresses in the scale. Notably, the stresses also increase gradually with oxidation time in contrast with previously reported piezospectroscopic measurements of the stress in scales on NiAl [32] and Ni<sub>3</sub>Al [27] alloys.

Converting the stress measurements to strain, the strain in the scale after 100 h at 1100°C is calculated to be 0.735% (compressive). This compares well with the value obtained by Luthra and Briant [12] using X-ray residual stress measurements on a similar material containing 0.3% Y. They made no measurements on a Y-free alloy. They found that their scales had a compressive strain of 0.776% after 72 h oxidation at 1225°C ( $\sigma = 4.1$  GPa for  $E = 373$  GPa and  $\nu = 0.3$ ) [12]. Their somewhat higher value is consistent with the increase in thermal expansion mismatch due to the higher oxidation temperature in their study. Since both values are higher than that expected from thermal expansion mismatch alone, it can be concluded that the scales in this alloy experience considerable compressive growth stresses during oxidation.

##### 4.2. Fe-Ni-Cr-Al alloys

There are very large differences in the compressive stress in the oxide scale formed on the yttrium-containing and yttrium-free Fe-Ni-Cr-Al materials after 1 h oxidation at the temperatures shown in Fig. 2. These differences disappear with longer oxidation times, Fig. 3, but after periods of longer than 10 h the scale of the yttrium-free alloy begins to spall preventing comparisons at much longer times. Interestingly, the regions of scale on the yttrium-free alloy that remain fully intact exhibit as large a residual stress as the yttrium-containing scale. Furthermore, with increasing oxidation time, the average stress in the regions of adhering scale on the yttrium-free alloy decreases presumably as microscopic decohering regions of the interface grow prior to scale spalling. This is believed to be the explanation for the very small values of the residual stress, much smaller than that of thermal mismatch, shown after 200 h in Fig. 3.

Both alumina and chromia form during oxidation of Fe–Ni–Cr–Al, but the alloy with yttrium forms significantly more alumina than chromia during 1 h of oxidation compared with the yttrium-free alloy, indicating an enhancement of the formation of alumina. In the yttrium-free material, the alumina passivation layer may not be completely formed, giving rise to lower compressive thermal stress than expected. A porous or incompletely formed alumina layer would have a smaller effective elastic modulus which would decrease the stress due to thermal expansion mismatch (equation 1). The thinner oxide scales on the yttrium-containing material could be attributed to the more quickly formed alumina passivation layer.

Comparison can be made with the data obtained on similar alloys by Huntz *et al.* [9] who used a beam deflection technique to monitor the growth stress during oxidation at 1000°C. From their deflection measurements, Huntz *et al.* deduced that the yttrium-containing scales were under 80 MPa compression after ~1 h oxidation as compared to about 400 MPa compressive stress in the yttrium-free alloy. This is in contrast to the results presented here which indicate that the stress in the scales on the yttrium-containing alloy are considerably higher than that in the yttrium-free alloy. In fact, using the calculated thermal expansion mismatch stress shown in Fig. 3, the growth stress in the scale on the yttrium-containing alloy would be at least 400 MPa compression whereas the stress in the scale on the yttrium-free alloy would be at least 1 GPa tension. The beam deflection values cannot, unfortunately, be directly compared to the piezospectroscopic measurements since the latter are of the stress in the alumina scale alone after cooling to room temperature. The difference, however, probably lies in the fact that the beam deflection method measures the composite stress due to both chromia and alumina formation during oxidation. So, if the majority of the growth stresses occur in the outer chromia layer rather than in the alumina layer, the chromia stress would dominate the beam deflection measurements. However, with longer times as the proportion of alumina in the scale increases and the stress in the alumina phase becomes dominant, one would expect the values from the two techniques to converge.

#### 4.3. Ni–Cr–Al alloys

The surprising result obtained from the scales formed on the Ni–Cr–Al alloys was that, except at 1225°C and long oxidation times, the stress was always less compressive than that expected from the thermal expansion mismatch (Fig. 4). This unexpected result is probably due to the formation of intermediate aluminum oxides in the scales at short times and low temperatures. Evidence for this comes from the observation that the fluorescence spectra recorded from the scales not only contained the R-line doublet characteristic of  $\alpha$ -Al<sub>2</sub>O<sub>3</sub> but also a

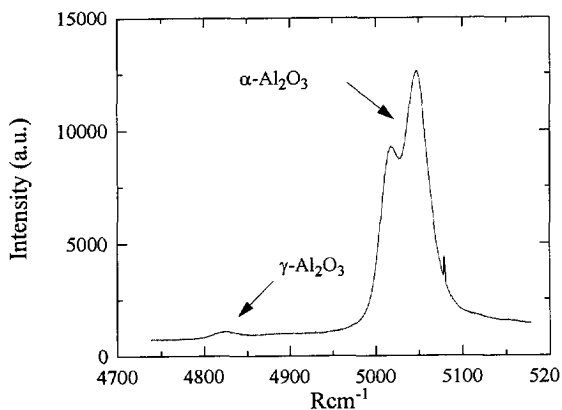


Fig. 6. Portion of the fluorescence spectra recorded from the scale on the Ni–Cr–Al (Y) alloy after 1 h oxidation in air at 950°C. In addition to the R-line doublet characteristic of alpha-alumina, the spectra exhibits a weaker fluorescence line believed to be due to the presence of an intermediate alumina phase, termed here  $\gamma$ , in the oxide scale.

weaker line which we have attributed to the presence of an intermediate polymorph, probably  $\gamma$ -Al<sub>2</sub>O<sub>3</sub>, in the oxide scale [34]. An example of the spectra obtained is shown in Fig. 6. For the alloys oxidized for 1 h at 950°C, both the scales from the yttrium-containing and yttrium-free alloys were found to contain the  $\gamma$ -Al<sub>2</sub>O<sub>3</sub> with the yttrium-containing alloy having rather more intense gamma peaks. In contrast with all the other results presented in this work, the stress in the scales formed on the yttrium-containing alloys was less compressive than the yttrium-free alloys when oxidized at 950 and 1050°C. The origin of the lower compressive stresses in the scales on these Ni–Cr–Al alloys is proposed to be a consequence of the volumetric decrease associated with the phase transformation from  $\gamma$ -Al<sub>2</sub>O<sub>3</sub> to  $\alpha$ -Al<sub>2</sub>O<sub>3</sub>. Typically during oxidation of alumina-forming alloys, such as these, intermediate forms of alumina, such as  $\gamma$ -Al<sub>2</sub>O<sub>3</sub>, form prior to the formation of the protective  $\alpha$ -Al<sub>2</sub>O<sub>3</sub> phase. In this particular Ni–Cr–Al alloy, the transformation seems to progress rather slowly. A volume decrease occurs when  $\gamma$  transforms to  $\alpha$  which would, in turn, cause a tensile stress in the constrained oxide. When added to the compressive thermal expansion mismatch stress, the net residual stress in the scale at room temperature would be less compressive and could account for the rather low values of the compressive stress at the lower temperatures. As the temperature and oxidation time increases, nearly all of the  $\gamma$ -Al<sub>2</sub>O<sub>3</sub> transforms and the residual stress approaches the expected value from the thermal mismatch stress prediction as seen after oxidation of the yttrium-containing alloys at 1225°C and at 1150°C after 100 h. The effect might be expected to be seen in the scales on the yttrium-free alloys but as indicated they spalled easily at 1150°C.

In contrast to our measurements of the stress in the scale on the yttrium-containing alloy, Luthra

and Briant [12] found that the stress in the scale on a very similar alloy, Ni-20 Cr-12.5 Al-0.3 Y formed at 1150°C after 96 h, was low. For commercial purity material they determined the stress at room temperature to be ~100 MPa (compressive) whereas the stress in the scale on high-purity material under the same conditions was ~255 MPa and tensile. They cited difficulties in making the measurements due to the weakness of the X-ray peaks.

### 5. IMPLICATIONS OF YTTRIUM ADDITIONS

Contrary to a number of hypotheses advanced for the role of reactive elements, the stress in the scales formed on yttrium-containing alloys is not lower than that on the yttrium-free alloys. Rather, the residual stress is generally higher in the scales formed on the yttrium-containing alloys. This is probably attributable to a higher creep relaxation stress of the scale formed on the yttrium-containing alloys as a result of either the alumina scale being more columnar or the grain boundaries in the scale being doped with yttrium. The instances in which the stress in the scales formed on yttrium-containing alloys was lower than those at short oxidation times when an intermediate alumina was still present in the scale. The lower stress in these instances is likely to be the result of the tensile stresses accompanying the constrained  $\gamma$ -to- $\alpha$  alumina transformation, rather than a direct result of the presence of yttrium. Indeed, such diminished compressive stresses have also been noted in scales formed on yttrium-free NiAl at short oxidation times when  $\gamma$ -alumina formed [32]. As the residual stress is not lower at longer times in the scales formed on yttrium-containing alloys it suggests that the most likely role of yttrium is to limit the degradation in interface fracture resistance that leads to the onset of spalling. Whether this is by combining with potential segregants that might weaken the alloy/scale interface or by limiting interfacial diffusion that promotes void growth or interface wrinkling, the role of yttrium influences the resistance to fracture rather than by decreasing the elastic strain energy release rate that would drive spalling.

### REFERENCES

1. W. T. Griffiths and L. B. Pfeil, U.K. Patent Number 459848, 1937.

2. *The Role of Active Elements in the Oxidation Behavior of High Temperature Metals and Alloys* (edited by E. Lang). Elsevier Applied Science, London (1989).
3. J. K. Tien and F. S. Petit, *Metall. Trans.* **3**, 1587 (1972).
4. J. D. Kuenzly and D. L. Douglass, *Oxid. Met.* **8**, 139 (1974).
5. F. A. Golightly, F. H. Stott and G. C. Wood, *Oxid. Met.* **10**, 163 (1976).
6. F. A. Golightly, F. H. Stott and G. C. Wood, *J. Electrochem. Soc.* **126**, 1035 (1979).
7. D. P. Whittle and J. Stringer, *Phil. Trans. R. Soc. Lond. A* **295**, 309 (1980).
8. F. A. Golightly, G. C. Wood and F. H. Stott, *Oxid. Met.* **14**, 217 (1980).
9. D. Delaunay, A. M. Huntz and P. Lacombe, *Corr. Sci.* **20**, 1109 (1980).
10. T. A. Ramanarayanan, M. Raghavan and R. Petkovic-Luton, *Oxid. Met.* **22**, 83 (1984).
11. A. B. Anderson, S. P. Mehandru and J. L. Smialek, *J. Electrochem. Soc.* **132**, 1695 (1985).
12. K. L. Luthra and C. L. Briant, *Oxid. Met.* **26**, 397 (1986).
13. J. G. Smeggil, A. W. Funkenbusch and N. S. Bornstein, *Metall. Trans. A* **17A**, 923 (1986).
14. A. M. Huntz, *Mater. Sci. Eng.* **87**, 251 (1987).
15. J. Jedlinski and S. Mrowec, *Mater. Sci. Eng.* **87**, 281 (1987).
16. A. M. Huntz, *et al.*, *App. Surf. Sci.* **28**, 345 (1987).
17. T. A. Ramanarayanan, R. Ayer, R. Petkovic-Luton and D. P. Leta, *Oxid. Met.* **29**, 445 (1988).
18. P. A. van Manen, *et al.*, *Surf. Interface Anal.* **12**, 391 (1988).
19. A. M. Huntz, *Mater. Sci. Tech.* **4**, 1079 (1988).
20. K. L. Luthra and C. L. Briant, *Mater. Sci. Forum* **43**, 299 (1989).
21. R. Prescott and M. J. Graham, *Oxid. Met.* **38**, 233 (1992).
22. D. R. Sigler, *Oxid. Met.* **40**, 555 (1993).
23. V. K. Tolpygo and H. J. Grabke, *Oxid. Met.* **41**, 343 (1994).
24. A. Aubry, *et al.*, *Acta Metall.* **36**, 2779 (1988).
25. A. Norin, *Oxid. Met.* **9**, 259 (1975).
26. D. M. Lipkin and D. R. Clarke, *Oxid. Met.* **45**, 267 (1995).
27. R. J. Christensen, D. M. Lipkin and D. R. Clarke, *Acta Metall. Mat.* **44**, 3813 (1995).
28. J. He and D. R. Clarke, *J. Amer. Ceram. Soc.* **78**, 1347 (1995).
29. Q. Ma and D. R. Clarke, *J. Amer. Ceram. Soc.* **76**, 1433 (1993).
30. *Thermophysical Properties of Matter, The TPRC Data Series* (edited by Y. S. Touloukian). **13**, IFI/Plenum, New York (1977).
31. P. A. Siemers and R. L. Mehan, *Ceramic Engineering and Science Proc.* **4**, 828 (1983).
32. D. M. Lipkin, D. R. Clarke, M. Hollatz, M. Bobeth and W. Pompe, *Corrosion Science*, In press.
33. L. Grabner, *J. Appl. Phys.* **49**, 580 (1978).
34. D. M. Lipkin, Q. Wen and D. R. Clarke, to be published.